

Relativistic plasma control for single attosecond x-ray burst generation

T. Baeva,^{1,*} S. Gordienko,² and A. Pukhov¹

¹*Institut für Theoretische Physik I, Heinrich-Heine-Universität Düsseldorf, D-40225, Germany*

²*L. D. Landau Institute for Theoretical Physics, Moscow, Russia*

(Received 9 January 2006; revised manuscript received 2 November 2006; published 5 December 2006)

We show that managing time-dependent polarization of the relativistically intense laser pulse incident on a plasma surface allows us to gate a single (sub)attosecond x-ray burst even when a multicycle driver is used. The single x-ray burst is emitted when the tangential component of the vector potential at the plasma surface vanishes. This relativistic plasma control is based on the theory of relativistic spikes [T. Baeva, S. Gordienko, and A. Pukhov, Phys. Rev. E **74**, 046404 (2006)]. The relativistic plasma control is demonstrated here numerically by particle-in-cell simulations.

DOI: [10.1103/PhysRevE.74.065401](https://doi.org/10.1103/PhysRevE.74.065401)

PACS number(s): 42.65.Ky, 52.27.Ny

High harmonics generated at plasma surfaces in the relativistic regime [1–7] are a promising new source of short wavelength radiation and attosecond pulses, necessary for the study of ultrafast processes in atoms, molecules, and solids at intensities significantly higher than those obtained from strong field laser-atom interactions [8,9].

The plasma harmonics are generated in the relativistic regime, when the laser pulse intensity $I \gg 10^{18}$ W/cm². Laser pulses in this intensity range usually are several cycles long. As a consequence, the reflected radiation contains a comb of attosecond pulses (*x* bursts). Yet, applications like molecular imaging [9,10] or quantum control [11] usually require a single short pulse to prevent undesirable effects, e.g., Coulomb explosion. The single attosecond pulse can be selected using a phase-stabilized single cycle laser [8]. An elegant way to control the atomic response by time-dependent laser polarization has been proposed earlier by Ivanov *et al.* in the context of gas harmonics [12].

In the present work, we show that the managed time-dependent polarization of the incident laser pulse allows us to gate a single (sub)attosecond pulse from the relativistically driven plasma surface in a well controlled way. Physically, the laser pulse polarization controls the relativistic γ -factor of the apparent reflection point (ARP) as seen by an external observer. Although the driving laser pulse can be long and intense, the ARP velocity becomes highly relativistic only when the vector potential component tangential to the plasma surface vanishes. At this moment, the single attosecond pulse is emitted. The time-dependent polarization corresponds to two perpendicularly polarized laser pulses with slightly different frequencies and a well chosen phase shift; see Fig. 1. Experimentally, the time-dependent laser pulse ellipticity can be achieved by the femtosecond polarization pulse shaping techniques [13].

We consider the interaction of an ultraintense short laser pulse with a slab of overdense plasma. We suppose that the plasma ions are immobile during the short interaction time and study the electron fluid oscillations only. It was shown in [4] that to describe the high harmonic generation analytically, the boundary condition

$$\mathbf{E}_\tau = 0 \quad (1)$$

must be used. Here \mathbf{E}_τ is the tangential to the plasma surface component of a constructed electric field, which coincides with the physical electric field outside the plasma and satisfies the vacuum wave equation everywhere. Of course, the constructed electric field differs from the real electric field inside the plasma slab. Yet this construction is sufficient to obtain all the information about the high harmonic spectrum [1].

The boundary condition (1) being stated for the constructed field is exact, which would not be the case for the physical (real) electric field. The difference between the physical and the constructed field can be seen if we consider the steady-state reflection of an electromagnetic wave on an ideal collisionless plasma: The energy absorption is zero, but the physical electric field $\mathbf{E}_{\text{physical}}$ vanishes only at infinity, so no point where $\mathbf{E}_{\text{physical}} = 0$ at any time is defined. At the same time, the constructed field (1) turns zero within the skin depth.

The physical meaning of the boundary condition (1) becomes clear if we consider the Poynting vector $\mathbf{S} = c\mathbf{E} \times \mathbf{B}/4\pi$ of electromagnetic energy flux. In the vacuum region in front of the plasma, it consists of incident flux $\mathbf{S}^i = c\mathbf{E}^i \times \mathbf{B}^i/4\pi$ and a reflected one $\mathbf{S}^r = c\mathbf{E}^r \times \mathbf{B}^r/4\pi$. Because the plasma slab is overdense, $\mathbf{S} = 0$ behind it. Neglect-

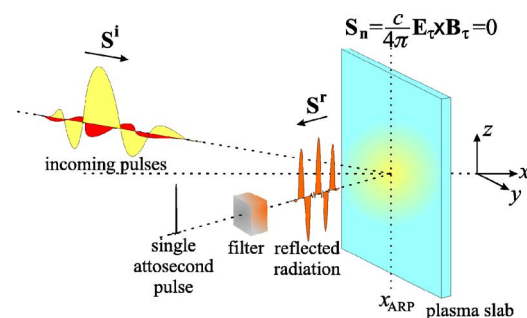


FIG. 1. (Color online) Geometry for relativistic plasma control of attosecond plasma surface dynamics. The high intensity driving pulse is polarization managed through a low intensity controlling pulse. After filtering of the reflected radiation, a single attosecond pulse can be isolated.

*Electronic address: tbaeva@tpl.uni-duesseldorf.de

ing the small absorption, the observer sees the apparent reflection at the point $x_{\text{ARP}}(t)$, where the normal component of the Poynting vector $\mathbf{S}_n = c\mathbf{E}_\tau \times \mathbf{B}_\tau / 4\pi = 0$. Thus the boundary condition (1) ensures energy conservation. The detailed microscopic derivation of the boundary condition $\mathbf{E}_\tau(x_{\text{ARP}}) = 0$ and its relation to the electron dynamics can be found in [14].

The incident laser field in vacuum runs in the positive x direction, $\mathbf{E}^i(x, t) = \mathbf{E}^i(x - ct)$, while the reflected field is translated backwards: $\mathbf{E}^r(x, t) = \mathbf{E}^r(x + ct)$. The tangential components of these fields interfere destructively at the ARP position $x_{\text{ARP}}(t)$, so that the implicit equation for the apparent reflection point $x_{\text{ARP}}(t)$ is

$$\mathbf{E}_\tau^i(x_{\text{ARP}} - ct) + \mathbf{E}_\tau^r(x_{\text{ARP}} + ct) = 0. \quad (2)$$

We stress that Eq. (2) contains the electromagnetic fields in vacuum. That is why the reflection point x_{ARP} is *apparent*. The real interaction within the plasma skin layer can be very complex. Yet, an external observer, who has information about the radiation in vacuum only, sees that $\mathbf{E}_\tau = 0$ at x_{ARP} . The ARP is located within the skin layer at the electron fluid surface, which is much shorter than the laser wavelength for overdense plasmas.

The ARP dynamics completely defines the high harmonic generation. In the ultrarelativistic regime, when the dimensionless vector potential $a_0 = eA_0/mc^2$ of the laser is large, $a_0^2 \gg 1$, we can apply ultrarelativistic similarity theory [15,16] to characterize this motion. The basic statement of this theory is that when we change the plasma density N_e and the laser amplitude a_0 simultaneously keeping the similarity parameter $S = N_e/a_0N_c$ constant the laser-plasma dynamics remains similar [17]. Here $N_c = \omega_0^2 m / 4\pi e^2$ is the critical plasma density for the laser pulse with the frequency ω_0 . This means that for different interactions with the same similarity parameter $S = \text{const}$, the plasma electrons move along the same trajectories, while their momenta \mathbf{p} scale with the laser amplitude: $\mathbf{p} \propto a_0$. Consequently, the electron momentum components tangential and normal to the plasma surface scale simultaneously with a_0 : $\mathbf{p}_\tau \propto a_0$; $\mathbf{p}_n \propto a_0$. Therefore, in general, the total electron momenta are not perpendicular to the surface. Moreover, the characteristic angle between their direction and the surface normal does not depend on a_0 provided that S is fixed.

This result is crucial for the plasma surface dynamics. It was shown in [1] by means of simple algebra that although the skin layer electrons move with ultrarelativistic velocities almost all the time for $a_0^2 \gg 1$, the relativistic γ -factor of the plasma surface and its velocity $v_s(t)$ behave in a quite different way. While the velocity is a smooth function of time with parabolalike maxima, the γ -factor of the boundary shows characteristic spikes of the order of a_0 for those moments of time t_g when $p_\tau(S, t_g) = 0$. The high harmonics are generated at the spikes, when the surface velocity is negative (plasma moving towards the laser pulse) and close to $-c$. The width of a γ -spike can be estimated as $\Delta t \propto 1/(\omega_0 \sqrt{\alpha} \gamma_{\text{max}})$, where α is a parameter dependent on S only, and connected to the plasma boundary acceleration. The (sub)attosecond x-ray

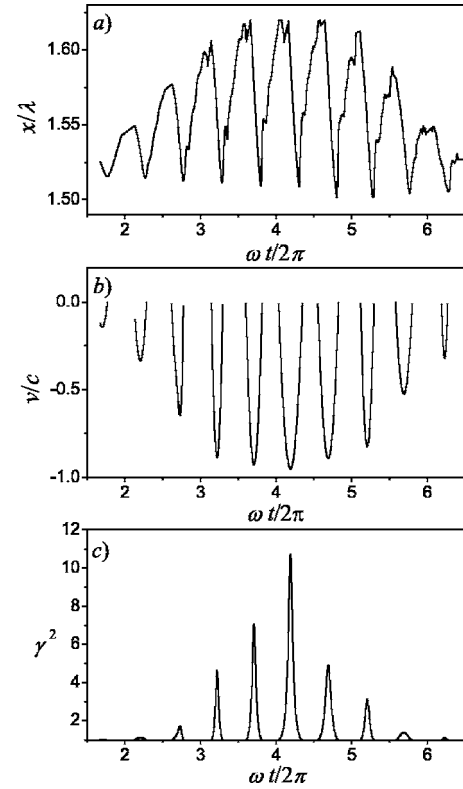


FIG. 2. 1D PIC simulation results for the parameters $a_0=20$ and $N_e=90N_c$. (a) Oscillatory motion of the point $x_{\text{ARP}}(t)$ where $\mathbf{E}_\tau(x(t))=0$. (b) Velocity $v_{\text{ARP}}(t)=dx_{\text{ARP}}(t)/dt$; only the negative velocities are shown. Notice that the ARP velocity is a smooth function around its maxima. (c) The corresponding γ -factor $\gamma_{\text{ARP}}(t)=1/\sqrt{1-v_{\text{ARP}}(t)^2/c^2}$ contains sharp spikes, which coincide with the velocity extrema.

bursts [4] are emitted exactly at the times of the spikes. The shortest attainable x-burst scales as

$$\tau_x \propto 1/(\omega_0 \gamma_{\text{max}}^3). \quad (3)$$

This favorable γ_{max}^{-3} scaling of the x-burst duration is due to the γ -spikes in the plasma surface dynamics.

We study the motion of the plasma boundary and the specific behavior of v_{ARP} and γ_{ARP} numerically using the 1D particle-in-cell (PIC) code VLPL [18]. The plasma slab is initially positioned between $x_L=1.5\lambda$ and $x_R=3.9\lambda$, where $\lambda=2\pi/\omega_0$ is the laser wavelength. The laser pulse has the Gaussian envelope $a(x, t=0)=a_0 \exp(-x^2/\sigma^2)\cos(2\pi x/\lambda)$, with $\sigma=2\lambda$.

At every time step, the incident and the reflected fields are recorded at $x=0$. Being solutions of the wave equation in vacuum, these fields can be easily chased to arbitrary x and t . To find the ARP position x_{ARP} , we solve Eq. (2) numerically. The trajectory of $x_{\text{ARP}}(t)$ for the simulation parameters $a_0=20$ and $N_e/N_c=90$ ($S=4.5$) is presented in Fig. 2(a). One can clearly see the oscillatory motion of the point $x_{\text{ARP}}(t)$. The equilibrium position is displaced from the initial plasma boundary position x_L due to the mean laser light pressure.

Since only the ARP motion towards the laser pulse is of importance for the high harmonic generation, we cut out

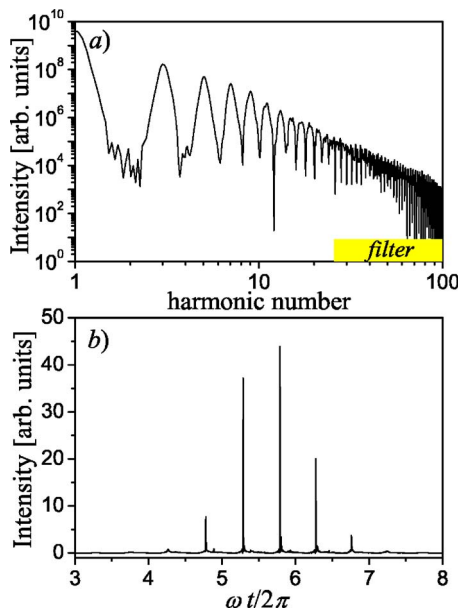


FIG. 3. (Color online) (a) The high harmonics spectrum; (b) the train of attosecond pulses is obtained after the proper filtering.

the positive ARP velocities $v_{\text{ARP}}(t) = dx_{\text{ARP}}(t)/dt$ and calculate only the negative ones, Fig. 2(b), because in our geometry negative velocity corresponds to motion towards the laser pulse. The corresponding γ -factor $\gamma_{\text{ARP}}(t) = 1/\sqrt{1-v_{\text{ARP}}(t)^2/c^2}$ is presented in Fig. 2(c). Notice that the ARP velocity is a smooth function around its maxima, resembling a parabola rather than a flat plateau. At the same time, the γ -factor $\gamma_{\text{ARP}}(t)$ contains sharp spikes, which coincide with the velocity extrema. These spikes of the surface γ -factor are responsible for the high harmonic generation.

The numerically obtained spectrum of the high harmonics is shown in Fig. 3(a). Filtering out the lower harmonics and keeping only the harmonics with $\omega > 25\omega_0$, we obtain a train of short pulses in the reflected radiation; see Fig. 3(b).

We have shown above that the attosecond pulses are emitted when the tangential components of the surface electron momentum vanish. This property can be used to control the high harmonic generation and to gate a particular attosecond pulse out of the train.

In the 1D geometry, the transverse generalized momentum is conserved: $\mathbf{p}_\tau = e\mathbf{A}_\tau/c$, where \mathbf{p}_τ and \mathbf{A}_τ are the tangential components of the electron momentum \mathbf{p} and the vector potential \mathbf{A} . Consequently, the attosecond pulses are emitted when the vector potential is zero. If the vector potential vanishes at several moments, there are several γ spikes and correspondingly, several short pulses are observed in the reflected radiation, see Fig. 3(b). To select a single attosecond pulse, we must ensure that the vector potential \mathbf{A}_τ turns zero exactly once. Since \mathbf{A}_τ has two components, how often it vanishes depends on its polarization. For linear polarization it vanishes twice per laser period, while for elliptic polarization it never equals zero. A laser pulse with time-dependent polarization can be prepared in such a way that its vector potential turns zero just once. A pulse of time-dependent polarization can be equivalently represented as a superposition of two perpendicularly polarized pulses, driv-

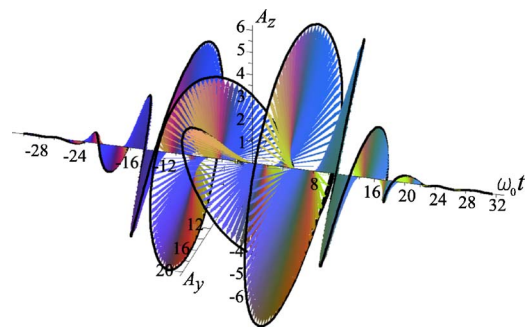


FIG. 4. (Color online) Vector potential of the polarization-managed laser pulse: Driver pulse with amplitude $a_0=20$, frequency $\omega_0=1$, and y polarization; z-polarized controlling pulse with amplitude $a_c=6$ and frequency $\omega_c=1.25$; phase shift $\Delta\phi=\pi/8$.

ing and controlling pulse, with slightly different frequencies and phases, see Fig. 1. Our PIC simulations suggest that a controlling signal with a few percent of the driver intensity is sufficient to manage the high harmonic generation, if the phase difference between the two laser pulses is chosen carefully.

To demonstrate the relativistic plasma control, we perform a PIC simulation where we add the z-polarized controlling pulse with amplitude $a_c=6$ and frequency $\omega_c=1.25$ and retain the same driver pulse with amplitude $a_0=20$, frequency $\omega_0=1$, and y polarization. We keep the same plasma density $N_e/N_c=90$. The optimal phase difference between the two lasers is found empirically to be $\Delta\phi=\pi/8$. The vector potential of the resulting laser pulse is represented as a function of time in Fig. 4.

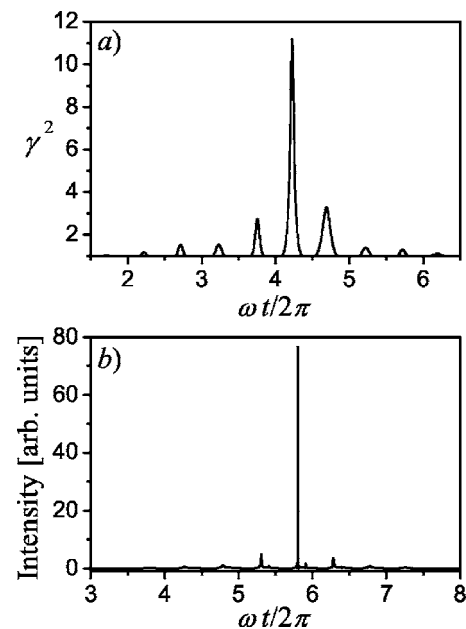


FIG. 5. Generation of a single attosecond pulse using the relativistic plasma control. The driver signal has $a_0=20$ and frequency $\omega_0=1$. The controlling signal has $a_c=6$ and frequency $\omega_c=1.25$. The phase difference is $\Delta\phi=\pi/8$. (a) The γ -spikes of the oscillating ARP; (b) the single attosecond pulse selected via the relativistic plasma control.

The simulation results are presented in Figs. 5(a) and 5(b). Comparing the surface γ -factor dynamics in the regime of linear polarization, Fig. 2(c), and in the controlled regime, Fig. 5(a), we see that the central γ -spike is slightly larger while both side spikes are significantly damped. This effect becomes much more pronounced when we compare the filtered radiation plots, Fig. 3(b) and Fig. 5(b). The control signal allows us to select the single attosecond pulse corresponding to the highest γ -spike in the surface motion.

Varying the control parameters a_0/a_c , ω_0/ω_c , and $\Delta\phi$ we are able to select different attosecond pulses one-by-one or in groups out of the original pulse train.

To recapitulate, we studied analytically and numerically the dynamics of the apparent reflection point at the

overdense plasma surface. The velocity of this point is a smooth function of time. The corresponding γ factor has spikes when the surface velocity approaches the speed of light. These ultrarelativistic spikes are responsible for the high harmonic generation in the form of an attosecond pulse train. We show that the attosecond pulse emission can be efficiently controlled by managing the laser polarization. This is done by adding a low intensity control pulse with perpendicular polarization and frequency slightly different from that of the driving pulse. This relativistic plasma control allows us to gate a single attosecond pulse or a prescribed group of attosecond pulses.

This work has been supported in part by DFG Transregio 18 and by DFG Graduierten Kolleg 1203.

-
- [1] T. Baeva, S. Gordienko, and A. Pukhov, Phys. Rev. E **74**, 046404 (2006).
 - [2] S. Kohlweyer *et al.*, Opt. Commun. **117**, 431 (1995); D. von der Linde *et al.*, Phys. Rev. A **52**, R25 (1995); P. A. Norreys *et al.*, Phys. Rev. Lett. **76**, 1832 (1996); M. Zepf *et al.*, Phys. Rev. E **58**, R5253 (1998); U. Teubner *et al.*, Phys. Rev. A **67**, 013816 (2003); I. Watts *et al.*, Phys. Rev. Lett. **88**, 155001 (2002); K. Eidmann *et al.*, Phys. Rev. E **72**, 036413 (2005).
 - [3] R. Lichters *et al.*, Phys. Plasmas **3**, 3425 (1996).
 - [4] S. Gordienko, A. Pukhov, O. Shorokhov, and T. Baeva, Phys. Rev. Lett. **93**, 115002 (2004).
 - [5] G. D. Tsakiris *et al.*, New J. Phys. **8**, 19 (2006).
 - [6] B. Dromey *et al.*, Nat. Phys. **2**, 456 (2006).
 - [7] A. Pukhov, Nat. Phys. **2**, 439 (2006).
 - [8] R. Kienberger and F. Krausz, Top. Appl. Phys. **95**, 343 (2004); E. Goulielmakis *et al.*, Science **305**, 1267 (2004); R. Kienberger *et al.*, Nature (London) **427**, 817 (2004).
 - [9] J. Itatani *et al.*, Nature (London) **432**, 867 (2004); H. Niikura *et al.*, Nature (London) **417**, 917 (2002).
 - [10] M. Lein, N. Hay, R. Velotta, J. P. Marangos, and P. L. Knight, Phys. Rev. A **66**, 023805 (2002).
 - [11] H. Rabitz *et al.*, Science **288**, 824 (2000); Y. Silberberg, Nature (London) **430**, 624 (2004).
 - [12] M. Ivanov, P. B. Corkum, T. Zuo, and A. Bandrauk, Phys. Rev. Lett. **74**, 2933 (1995).
 - [13] T. Brixner *et al.*, Phys. Rev. Lett. **92**, 208301 (2004).
 - [14] T. Baeva, Diploma thesis, Heinrich-Heine-University, 2005.
 - [15] S. Gordienko and A. Pukhov, Phys. Plasmas **12**, 043109 (2005).
 - [16] D. D. Ryutov and B. A. Remington, Plasma Phys. Controlled Fusion **48**, L23 (2006).
 - [17] A. Pukhov and S. Gordienko, Philos. Trans. R. Soc. London, Ser. A **364**, 623 (2006).
 - [18] A. Pukhov, J. Plasma Phys. **61**, 425 (1999).